

# What pp SUSY limits mean for future $e^+e^-$ colliders\*

Mikael Berggren

DESY, Notkestraße 85, D-22607 Hamburg -Germany

It is well-known that  $e^+e^-$  colliders have the power to with certainty exclude or discover any SUSY model that predicts a Next to lightest SUSY particle (an NLSP) that has a mass up to slightly below the half the centre-of-mass energy of the collider.

Here, we present an estimation of the power of present and future hadron colliders to extend the reach of searches for SUSY, with particular emphasis whether it can be claimed that either discovery or exclusion is *guaranteed* in a region of LSP and NLSP masses - no set of values of the other SUSY could change the conclusion. We study this by, reasonably, assuming that the most challenging scenario would be one where the lightest SUSY particles are the electroweak bosinos, and that sfermions are out of reach. A scan over SUSY parameter space was done, only requiring that the NLSP was a bosino with mass not larger than a few TeV. The mass-spectrum, cross-sections and decay branching ratios found in this region were confronted with projections of sensitivity at future hadron colliders. In our conclusions we weigh in the maturity of the analysis the projections are based upon. The conclusion is that although future hadron colliders have a large discovery-reach, i.e. potential to discover *some* SUSY model, hardly any models with low-to-medium LSP-NLSP mass-differences can be excluded with certainty. The models that are expected to be excluded/discovered are, on one hand, those with mass-differences larger than those allowed by models with GUT-scale  $M_1$ - $M_2$  unification, and on the other hand, a tiny region where the mass-difference is so small that the NLSP decays in the tracking volume of the detectors. Excluding the latter possibility does not, however, allow to exclude the possibility of a Wino or Higgsino LSP: at any value of the LSP mass, we could identify models where the NLSP lifetime would be too short for a signal to be seen.

## 1 Introduction: SUSY and future colliders

If Supersymmetry (SUSY) [1] is to explain the current problems of the Standard Model for particles physics, such as the naturalness of the theory, the hierarchy problem, the nature of Dark Matter, or the possible discrepancy between the observed and predicted value on the muon magnetic moment ( $g-2$ ), a light electroweak SUSY sector is preferred. From LEP II, it is known that an electroweak sector with masses below  $\sim 100$  GeV is excluded, except for some very special cases. From LHC, we know that a coloured sector with masses below  $\sim 1$  TeV is also excluded. However, except for the third generation squarks, the coloured sector does not contribute significantly to clarify the mentioned issues with the SM.

The model-space of the electroweak sector of SUSY can conveniently be sub-divided by the nature of the Lightest SUSY Particle (the LSP) as the Bino-, Higgsino- or Wino-region, defined by whether  $M_1$ ,  $\mu$ , or  $M_2$  is the smallest of the three, and thus which field is the largest contributor to the mass-eigenstate (not to be confused with *pure* Wino, Bino or Higgsino models, where the respective contributions are

---

\*Contribution to the International Workshop on Future Linear Colliders (LCWS2019), Sendai, Japan, 28 October-1 November, 2019. C19-10-28

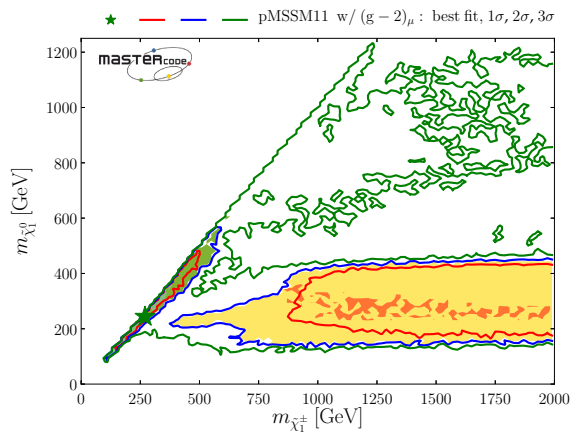
close to 100 %). Alternatively, one can classify by the size of the mass-difference,  $\Delta(M)$ , between the LSP and the next-to-lightest SUSY particle (the NLSP), as high  $\Delta(M)$  or low  $\Delta(M)$ . The first case coincides with the Bino-region, the second contains the Higgsino- and Wino-regions, which differ in important experimental consequences. In other words: In the Higgsino- and Wino-regions, the electroweak SUSY sector is “compressed”, i.e. the masses of some of the other electroweak bosinos tend to be close to the LSP mass. In this situation, most decays of massive sparticles are via cascades, and at the end of these cascades, the mass difference is small, in turn meaning that the final decay into the invisible LSP releases little energy. While such events show large missing energy, this is of no help at hadron colliders - contrary to the case at lepton colliders - since the initial energy is unknown. Therefore, to address such cases at hadron colliders, one must resort to missing transverse momentum, a much more delicate signal. Consequently, for such topologies, current limits from LHC are for specific models, and the results from LEP II [2–6] are those that yield the model-independent exclusions. The same observations are also valid if the NLSP is a slepton in general, and the  $\tilde{\tau}$  in particular.

The organisation of the note is as follows. We first discuss how to compare different options on an equal footing in section 2, and present our scan-range, tools and general observations about the mass-spectra in section 3. In section 4, we discuss the interpretation of the electroweak SUSY chapter of the physics Briefing-book [7] to the update of the European strategy for particle physics (the ESU) in view of our observations. In section 5, for reference, we summarise the ILC projections, before concluding in section 6.

## 2 Comparing options

For asserting the capabilities of future facilities to explore SUSY, it is important to make the distinction between discovery potential and exclusion potential. The former is power to discover *some* model, while the latter is the power to exclude *all* models compatible with the shown parameters, i.e. marginalising over all non-shown parameters. The methodologies needed in the two cases are different. In the first case, one would concentrate on specific models yielding signatures that are observable as far into uncharted territory as possible, while in the latter case one needs to determine which model is the most difficult, and evaluate whether that worst-case would be observed, if it is realised in nature. The latter was indeed the focus at LEP II. The limits from there have been marginalised over all other parameters, and can be considered definite.

A further consideration that must be made in weighing different future



(a)  $\mu$  vs.  $M_1$

Figure 1: pMSSM11 fit by MasterCode to LHC13/LEP/g-2/DM(=100% LSP)/precision observables in the  $M_{\tilde{\chi}_1^\pm} - M_{\tilde{\chi}_1^0}$  plane. From [8a].

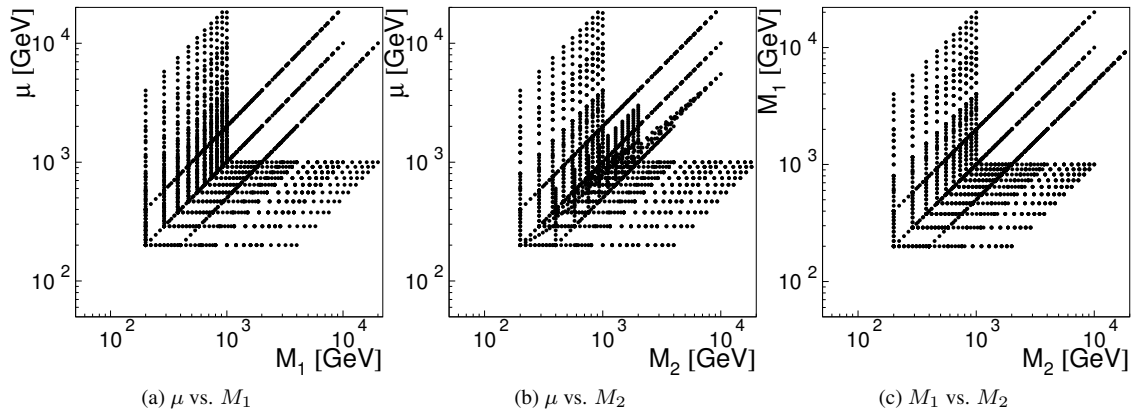


Figure 2: The scanned points in  $\mu$ ,  $M_1$  and  $M_2$ .

projects against each other is the level of understanding. This includes the level of maturity of the project, ranging from existing results (e.g. from LEP or LHC), over existing/in construction new detectors and machines (HL-LHC), TDR-level new facilities, such as ILC or CLIC, to conceptual extensions to existing facilities (HE-LHC, LHeC). It further extends to new conceptual ideas, such as the different options for FCC, and continues to emerging technologies, e.g. plasma acceleration or  $\mu$ -colliders. One must also consider the level of detail of studies done, which range from fully simulated, well defined detectors and accelerators (LHC, HL-LHC, ILC, and CLIC), fully simulated evolving concepts, e.g. CepC, over detailed fast simulation (i.e. with more detail than purely parametric simulations), to parametric simulations with parametric input from full simulation of the proposed detector, or simply using parameters from an existing detector at a new facility. Also pure four-vector smearing of generated objects and simple cross-section level estimates can be used as initial estimates. In the case of cross-section and luminosity scaling estimates, one should also consider whether they were done at the level of the final published exclusion reach, or had access to more basic information of the extrapolated experiment (background event count, efficiency tables etc.) Finally, when it comes to interpreting the results of such studies it is also important to consider whether they were done by detector experts or not. This is of particular importance for systematics-limited experiments, and cases where detailed knowledge of object-finding and reconstruction is essential.

### 3 Estimating SUSY reach

Several groups [8] have combined current experimental observations with SUSY theory to estimate where to in the parameter space observations point, and to estimate what regions actually are excluded at present. One example, from the MasterCode group [8a], is show as Figure 1. It, interestingly, indicates that current results point to the aforementioned “compressed region”. This type of studies aims at answering the question about where SUSY is most likely to be found, and to compare this with the estimated capabilities of present or future facilities and techniques. It should be noted that to arrive at definite conclusions, the analyses typically include non-HEP observations. Whether, and how, these can be put in to a HEP context already contains assumptions. E.g. it is often assumed that SUSY is the sole

source of WIMP dark matter, and that direct or indirect searches for WIMPs can be translated into HEP observations. However, other well motivated candidates for dark matter exists, the prime example being the QCD axion [9], so it might well be that SUSY is realised in nature, but is not the (full) explanation for Dark Matter. In addition, the estimates sometimes include results that hint to physics beyond the standard model, but that are not yet solidly established, g-2 of the muon being one example.

If one is interested in the *guaranteed* reach, rather than the *possible* reach, one should not rely on assumptions that are not directly testable. In essence, this means to concentrate on the *exclusion reach*. In SUSY, the fundamental principle that sparticles and particles have the same couplings and the same quantum-numbers (except for spin), sets a scene where such a program is possible. It implies that cross-sections and decay modes are completely know within SUSY itself. In particular, if R-parity conservation is assumed, it means that there is always one completely know process, namely NLSP production, followed by the decay of the NLSP to it's SM partner and the LSP, if kinematically allowed, with 100 % branching ratio. In estimating the exclusion reach, rather than the discovery reach, it is essential to find the *most challenging* situations. Such a scenario is easily found, and we will consider

- the MSSM with R-parity conservation, since LEP experience shows that the case of R-parity violation is always less demanding at  $e^+e^-$  machines, and likely to also be so at hadron machines.
- The NLSP is not a sfermion, for the same reason. The  $\tilde{\tau}$  is an exception, in that the LEP experience indicates that a  $\tilde{\tau}$  NLSP might be even more challenging than a bosino one. However, the issue is even more pronounced at a hadron collider [10].

Under these conditions both the LSP and the NLSP are more or less pure Binos, Winos, or Higgsinos, and  $M_1, M_2$  and  $\mu$  are the MSSM parameters most influencing the experimental signatures. We consider any values, and combinations of signs, of these parameters, up to values that makes the bosinos kinematically out-of-reach for any new facility, i.e. up to a few TeV. We also vary other parameters

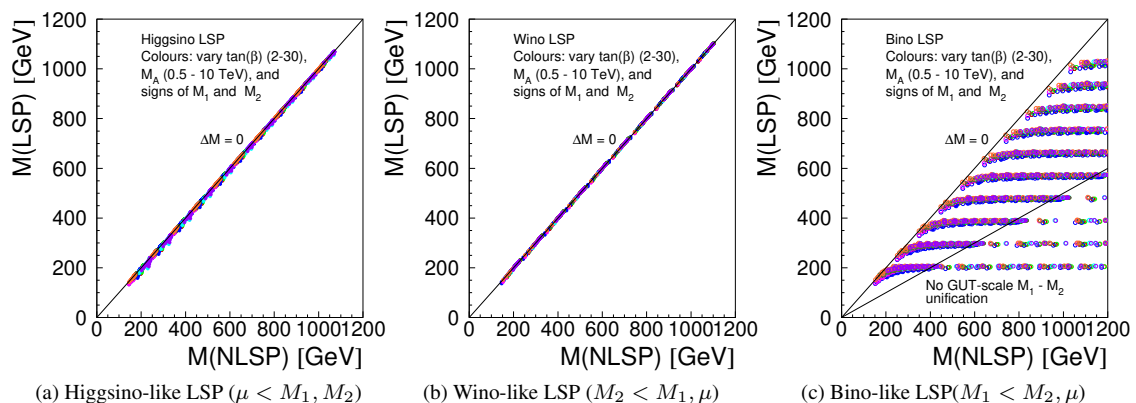


Figure 3: The LSP mass vs. the NLSP mass for the three cases. The colour coding is the following: Points with the same colour have varying values of the bosino parameters, as per Figure 2, while the colours are: All point have  $\tan \beta=10$ , except light green ( $\tan \beta=3$ ) and blue ( $\tan \beta=30$ ). All have  $M_A=5$  TeV except black ( $M_A=0.5$  TeV) and magenta ( $M_A=10$  TeV). All have positive sign of  $\mu, M_1$ , and  $M_2$ , except cyan (-,+), olive-green (+,+,-), orange (+,-,+), and purple (+,-,-). Open symbols are for  $|M_2 - 2M_1|/|M_1| > 0.1$  (i.e. not close to the GUT-unification case).

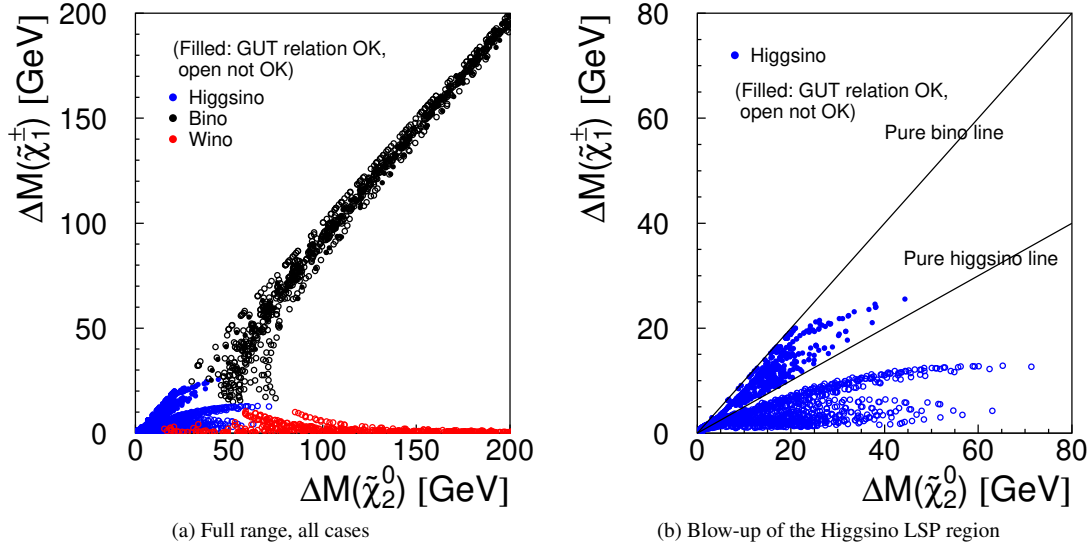


Figure 4: The mass difference between the LSP and  $\tilde{\chi}_1^\pm$  versus that between the LSP and  $\tilde{\chi}_2^0$ .

( $\tan \beta = 3$  to  $30$ ,  $M_A = 0.5$  to  $10$  TeV,  $M_{\text{fermion}} = 5$  to  $10$  TeV), to verify that they have only a minor impact on the signatures. No other assumptions, such as relations between the parameters due to some specific SUSY-breaking mechanism, are done. No assumption on prior probabilities is implied, and therefore that the density of points in the various projections that will be shown is not of great importance. The important observation to be made is whether *there are* any points outside excluded regions: this implies that the model *cannot* be excluded.

Figure 2 shows the points studied in  $M_1, M_2$  and  $\mu$  as three two-dimensional projections. We proceed to find what happens with spectra, cross-sections, and decay branching-ratios when exploiting this “cube”. In order to do so, `SPheno 4.0.5` [11] was used to calculate spectra and and decay branching ratios at each point, and `Whizard 2.8.0` [12] was used to find the production cross-sections, and to generate parton-level events. In addition `FeynHiggs 2.16.0` [13] was used to calculate the expected mass of the SM-like higgs boson, and as a double-check of the sparticle mass-spectrum. Around 80 % of the points had calculated higgs-mass agreeing with the experimental value at the  $2\sigma$  level of the theoretical uncertainty, with the exception of the points with the highest of the three  $\tan \beta$  values in our scan, namely  $\tan \beta = 30$ , where only 7, 9 and 23 % of the points were in the range for Wino-, Bino- and Higgsino-LSP, respectively. None of the features shown in the following figures, however, change if demanding that the calculated higgs-mass was in the two standard deviation range. The main features are shown in Figure 3. One observes that, except for Bino-LSP, the LSP-NLSP splitting is small. The colours indicate different settings of the secondary parameters; the observation is that they don’t matter much. In addition, the open circles indicate cases where GUT-scale unification of  $M_1$  and  $M_2$  is not possible<sup>1</sup>.

<sup>1</sup> If  $M_1$  and  $M_2$  are unified at the GUT scale, the different RGE running of the two results in the relation  $M_2 = (3g^2/5g'^2)M_1 \approx 2M_1$  at the weak scale. The maximally stretched difference between the LSP and the NLSP occurs when the LSP is pure Bino, and the NLSP a pure Wino. In this case  $M_{\text{LSP}} = M_1$  and  $M_{\text{NLSP}} = M_2 = 2M_1$ . A Higgsino admixture in these states can only make the difference *smaller*.

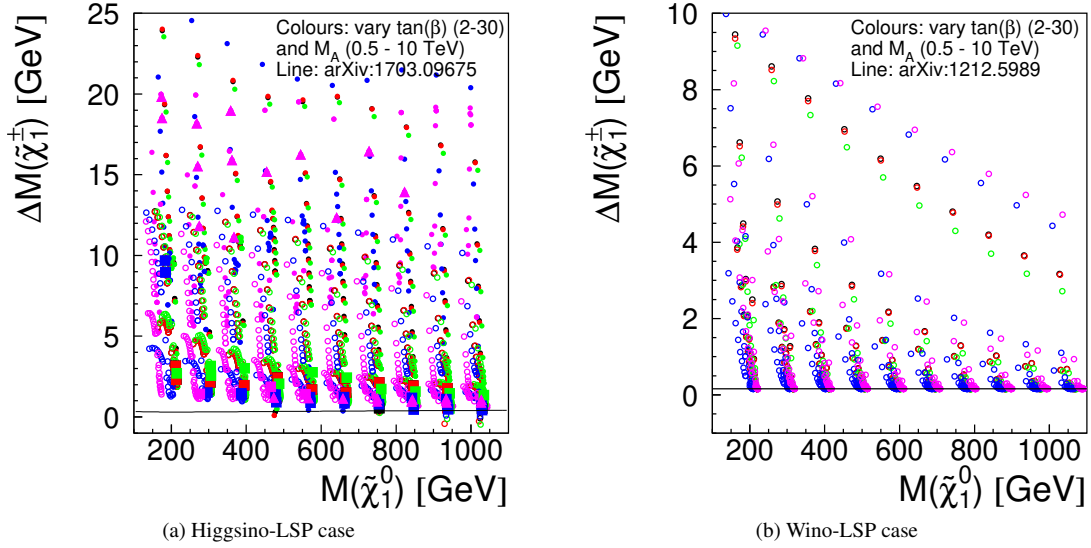


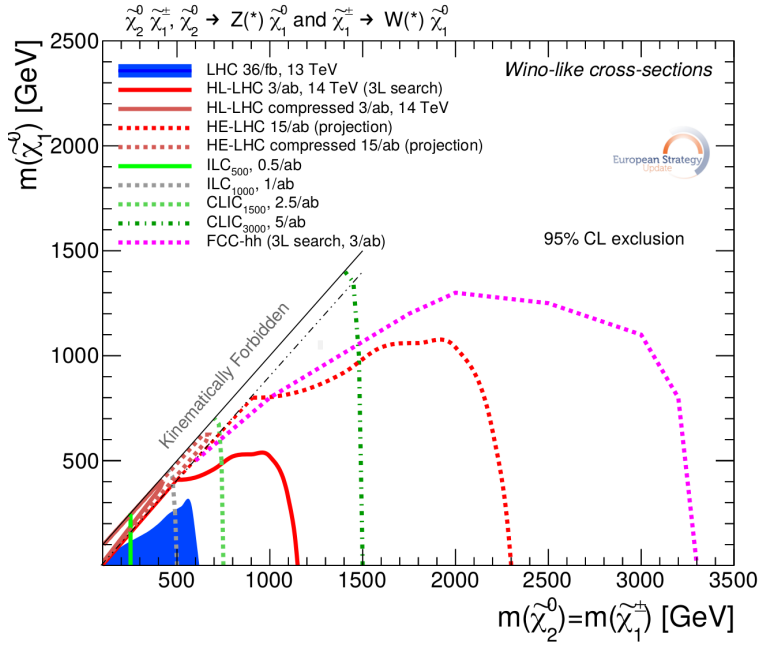
Figure 5:  $\Delta(M_{\tilde{\chi}_1^\pm})$  vs.  $M_{LSP}$  in the small  $\Delta(M)$  region. In (a), the squares are points where  $\Delta(M_{\tilde{\chi}_1^\pm}) \approx \Delta(M_{\tilde{\chi}_2^0})/2$ , and triangles are points where  $\Delta(M_{\tilde{\chi}_1^\pm}) \approx \Delta(M_{\tilde{\chi}_2^0})$ . Colours as explained in Figure 3.

In many models, the next-to-next lightest SUSY particle (the NNLSP) is close in mass to the NLSP. Therefore, another aspect of experimental importance is the mass-differences to the LSP of both the lightest chargino and of the second lightest neutralino: either of these could be either the NLSP or the NNLSP. This aspect is shown in Figure 4 which shows  $\Delta(M)$  for  $\tilde{\chi}_1^\pm$  versus that of  $\tilde{\chi}_2^0$ . One notes three distinct regions

- Bino LSP: Both mass differences quite similar, but can take any value;
- Wino LSP:  $\Delta(M_{\tilde{\chi}_1^\pm})$  will be small, while  $\Delta(M_{\tilde{\chi}_2^0})$  can vary largely;
- Higgsino LSP: Both mass differences often small.

Note, however, that in the Higgsino LSP case, few models are on the ‘‘Higgsino line’’, i.e. the case where the chargino is *exactly* in the middle of mass-gap between the first and second neutralino. Finally, Figure 5 show  $\Delta(M)$  for  $\tilde{\chi}_1^\pm$  vs.  $M_{LSP}$  for a Higgsino LSP or a Wino LSP. Here, one can note that in both scenarios, quite a large spread is possible, and that some Higgsino models actually have a chargino LSP. The last feature is a point of disagreement between the results of `SPheno` and `FeynHiggs` - the latter does not find models with a chargino LSP<sup>2</sup>.

<sup>2</sup>There are differences to be expected as in case of `SPheno` this is a pure  $\overline{\text{DR}}$  calculation whereas in `FeynHiggs` on-shell calculation is performed. This issue needs further investigation.



(a)

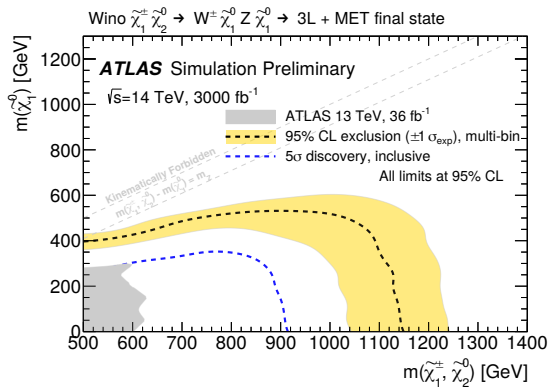
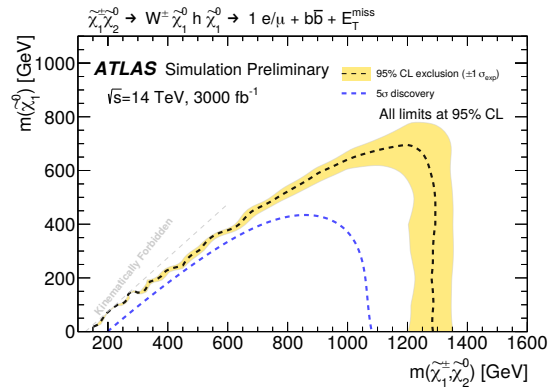
(b)  $\tilde{\chi}_1^\pm \rightarrow Z\tilde{\chi}_1^0$ (c)  $\tilde{\chi}_1^\pm \rightarrow h\tilde{\chi}_1^0$ 

Figure 6: The reaches in the high  $\Delta(M)$  (Bino-LSP) region, as reported in [7] (top), and the two projections to HL-LHC from ATLAS [14] (bottom). (b) corresponds to the solid red line in (a).

## 4 SUSY In the Briefing-book

In the physics Briefing-book of the update of the European strategy for particle physics [7], the reach of searches for electroweak SUSY particles for different proposed future accelerators are presented in chapter 8.3.2, and illustrated by two figures. We will discuss these in this section.

### 4.1 Bino LSP

Figure 8.9 in [7] (reproduced here as Figure 6) shows the estimated reaches in the Bino LSP case, i.e. for the large  $\Delta(M)$  case. The signature for this scenario at pp-colliders are events with large missing transverse momentum (MET). Due to the large mass-difference, the missing momentum originates from the invisible SUSY particles themselves, i.e. there is no need for a system recoiling against the SUSY particles. To first order, this makes the analyses robust, since only the mass-difference is needed to predict the signal topologies. However, there are still a number of model-dependencies, discussed below. The sources of the curves shown for the various pp options are from the projection to HL-LHC by the ATLAS collaboration [14]. The result presented in that publication is the solid red line in Figure 6a, and the actual plot from the paper is reproduced as Figure 6b. This curve is extrapolated giving the HE-LHC curve (red-dotted). Several things should be noted: The curve shown is the exclusion reach, not the discovery reach (for the CLIC and ILC curves, the differences between exclusion and discovery reach are less than the width of the lines in the figure). The ATLAS result is only shown down to  $M_{\tilde{\chi}_1^\pm} = 500$  GeV, the region below this is just a guide-the-eye straight line. The chosen decay-mode ( $\tilde{\chi}_1^\pm \rightarrow Z\tilde{\chi}_1^0$ ) is the most sensitive at low  $\Delta M$ . The other mode ( $\tilde{\chi}_1^\pm \rightarrow h\tilde{\chi}_1^0$ ), shown in Figure 6c is less powerful in this region. On the other hand the higgs mode is expected to probe higher  $M_{\tilde{\chi}_1^\pm}$  at the highest  $\Delta M$ . At CLIC or ILC, one does not need to make such a distinction. The issue of the dominant decay mode is important, as illustrated in Figure 7. In these figures, we show the branching ratios in Bino-LSP models (i.e. models where  $M_1$  is the smallest of the bosino parameters), when only the relative signs of  $M_1$ ,  $M_2$  and  $\mu$  are modified. The observation is that whether the  $Z$  or the  $h$  mode is dominant depends crucially of the choice of the relative sign, and hence that the exclusion-region should be the *intersection* of Figures 6b and c, not the *union*.

One can note that the exclusion region remains below a line with slope  $\sim 1/2$  when luminosity and/or energy is increased. The reason for this is as follows: Figure 8 shows how the cross-section varies with the sum of the two bosino masses at FCChh-conditions. Here a simple setup - which is nevertheless

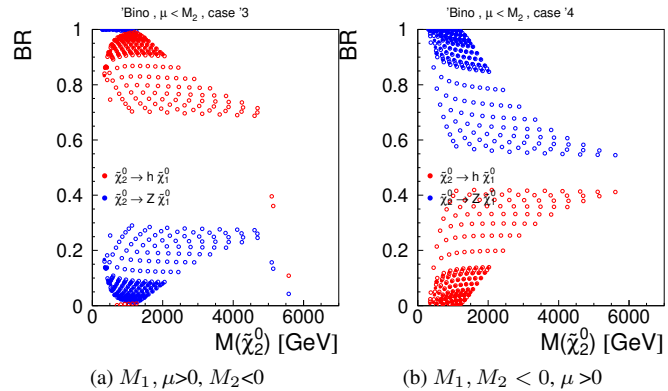


Figure 7: Branching ratios of  $\tilde{\chi}_1^\pm \rightarrow Z\tilde{\chi}_1^0$  (blue) and  $\tilde{\chi}_1^\pm \rightarrow h\tilde{\chi}_1^0$  (red) in the Bino LSP case, with  $|\mu| < |M_2|$ , and different signs of  $\mu$ ,  $M_1$ , and  $M_2$ . The same grid in absolute values of  $\mu$ ,  $M_1$ , and  $M_2$  is used in both (a) and (b).



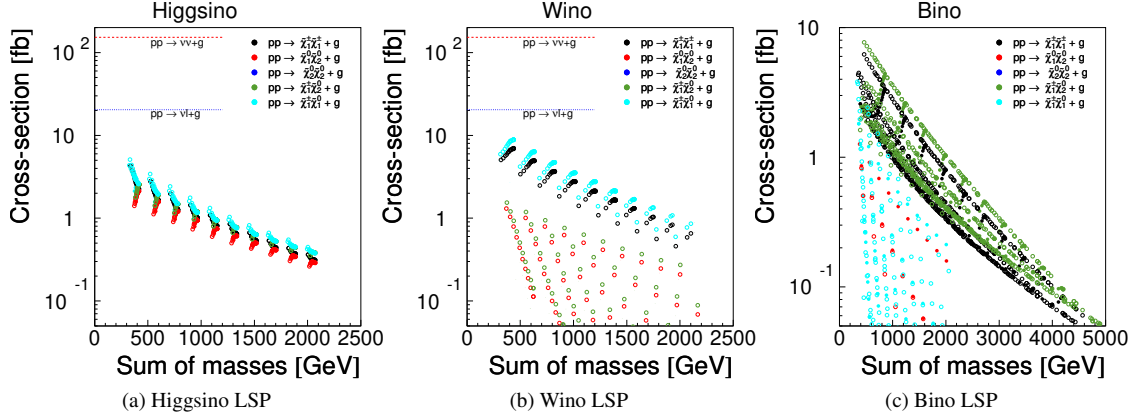


Figure 8: Cross sections for  $pp \rightarrow$  two uncoloured bosinos + a gluon, as a function of the sum of the masses of the two bosinos. The five different final states are shown separately, as indicated in the figures.

adequate for illustrating the scaling behaviour - was used to calculate cross-section  $\times$  branching-ratios using *Whizard*. The process is  $pp \rightarrow$  uncoloured bosinos + gluon, with the *Whizard*-default parton density function (CTEQ6L1[15]). Two observations can be made. Firstly, there is a close to exponential fall of the cross-section with mass. Secondly, the cross-section at any given mass can vary by a factor  $\sim 2$ , by varying the parameters of the model. The exponential fall-off with increasing mass comes around for the following reason: If the mass of the interacting quark-pair would be fixed (equivalent to the situation at a lepton collider, where the invariant mass of the initial state is fixed ( $= 2 \times E_{beam}$ )), the cross section versus the mass of the produced bosino pair initially rises proportionally to  $\beta$  - typical for fermion pair-production - followed by a fall-off proportional to  $\frac{1}{s}$ , see Figure 9a. Once this is folded with the distribution of  $m_{qq}$  given by the rapidly falling parton densities<sup>3</sup>, the actual distribution on  $m_{qq}$ , given that a bosino production took place shows a distribution - albeit broad - that correlates with the mass of the bosino pair (Figure 9b). This correlation is close to linear, as can be seen in 9c.

Generally, the maximum missing momentum due to the invisible LSPs is

$$\mathcal{R}_{max} = 2\gamma_{f\bar{f}}\beta_{f\bar{f}}\gamma_{NLSP}E_{LSP} + 2\gamma_{f\bar{f}}\gamma_{NLSP}p_{LSP} \quad (1)$$

In the Bino case, the initial  $f\bar{f}$ -system need not be boosted, so  $\gamma_{f\bar{f}}\beta_{f\bar{f}} \approx 0$ ,  $\gamma_{f\bar{f}} \approx 1$ ,  $\gamma_{NLSP} = E_{NLSP}/M_{NLSP} \approx M_{f\bar{f}}/2M_{NLSP}$  and

$$\mathcal{R}_{max} \approx 2\frac{M_{f\bar{f}}}{2M_{NLSP}}p_{LSP} \approx 2\frac{M_{f\bar{f}}}{2M_{NLSP}}\frac{M_{NLSP}^2 - M_{LSP}^2}{2M_{NLSP}} \quad (2)$$

where the last step is because at interesting points, the SUSY particle mass is much above it's SM partner (even if this is a  $W$ ,  $Z$  or  $h$ ). From Figure 9c, we know that  $M_{f\bar{f}} \approx 3M_{NLSP}$ , and

$$\mathcal{R}_{max} \approx \frac{3}{2}M_{NLSP}\left(1 - \left(\frac{M_{LSP}}{M_{NLSP}}\right)^2\right) \quad (3)$$

<sup>3</sup>Note that for the Drell-Yan production of the bosino pair, at least one of the partons must come from the sea

Hence, at these LSP-NLSP mass-ratios, the missing  $p_T$  due to the invisible LSP is proportional to the bosino-mass. This means that one can increase the missing  $p_T$  cut while conserving a given the signal efficiency as one searches for higher bosino masses. The missing  $p_T$  from irreducible background (typically Dell-Yan + gluon, with  $Z \rightarrow \nu\bar{\nu}$ ) is obviously independent for the bosino masses, but does depend on the required missing  $p_T$ , essentially the  $p_T$  of the gluon. Figure 10a shows that if the  $p_T$  cut applied is the one that keeps the same signal efficiency at any given  $M_{\tilde{\chi}_1^\pm}$ , the  $M_{f\bar{f}}$  of the background events passing the cut also follows a linear trend quite similar to that of the signal, seen in 9c. In the figure, the cut has been set to  $0.85 M_{\tilde{\chi}_1^\pm}$ , which according to Eq. 3 corresponds to  $0.75 \times$  the maximal missing  $p_T$  from  $\tilde{\chi}_1^\pm$  pair-production, when  $M_{NLSP} = 2M_{LSP}$ , as it is at the border of the currently excluded region. The cross-section for this process therefore also falls exponentially with the required  $p_T$ , (see Figure 10b) meaning that the signal-to-background ratio will remain constant along lines through the origin in the  $M_{\tilde{\chi}_1^\pm}$  vs.  $M_{LSP}$  plane. On the other hand, Eq. 3 also shows that the missing  $p_T$  decreases with increasing  $M_{LSP}/M_{NLSP}$ , meaning that to exclude lower  $\Delta(M)$  at the same efficiency requires a decrease in the cut, leading to a large increase in the background. Comparing the solid and dashed blue lines in Figure 10b shows that to half the excluded  $\Delta(M)$  at  $M_{\tilde{\chi}_1^\pm} = 2$  TeV would require  $\sim 10$  times more luminosity, assuming that no new background sources would start contributing (e.g. jet-energy resolution, jet-energy scale, non-direct neutrinos, etc.), which clearly is an unrealistic best-case.

To conclude this discussion of the Bino LSP case, we note that although the signal is robust, there are a number of issues that must be taken into account: The analyses are typically performed using a set of processes involving production of different combinations of LSPs, NLSPs and NNLSPs. The sensitivity is different for different channels, and Figure 8c shows that the cross-sections, and their ratios, can vary substantially between models. Furthermore, we also noted that the dominating decay mode of the second neutralino is strongly dependent on the relative signs of  $\mu, M_1$  and  $M_2$ , and that the sensitivity of the analyses depends also on this. To claim that an  $M_{NLSP}$ - $M_{LSP}$  is excluded, the

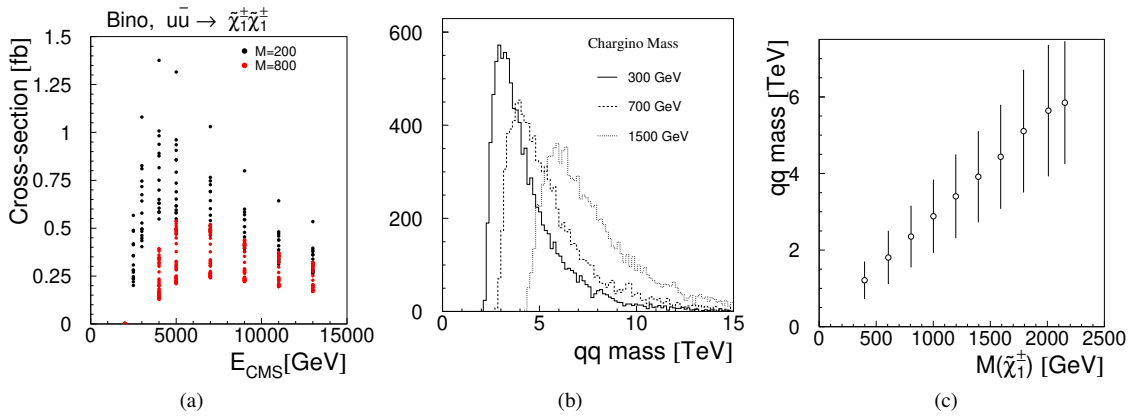


Figure 9: Properties of  $\tilde{\chi}_1^\pm$  production: (a) Cross-section at fixed  $m_{qq}$ ; (b) Distributions of  $m_{qq}$  at different  $M_{\tilde{\chi}_1^\pm}$  in pp; (c) Average  $m_{qq}$  vs.  $M_{\tilde{\chi}_1^\pm}$  in pp. The error-bars represent the r.m.s. of the distribution, not the r.m.s. of the mean.

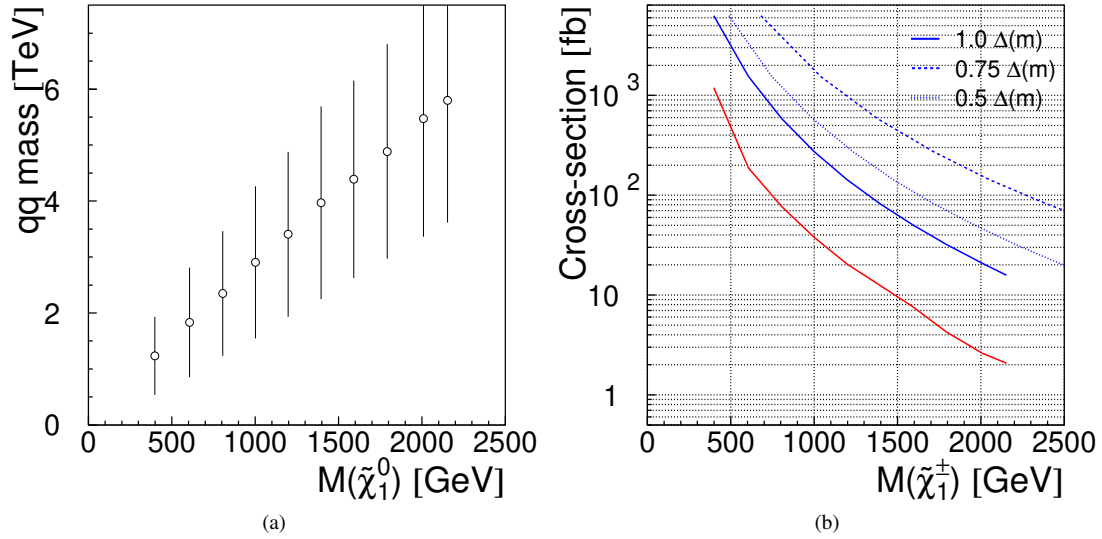
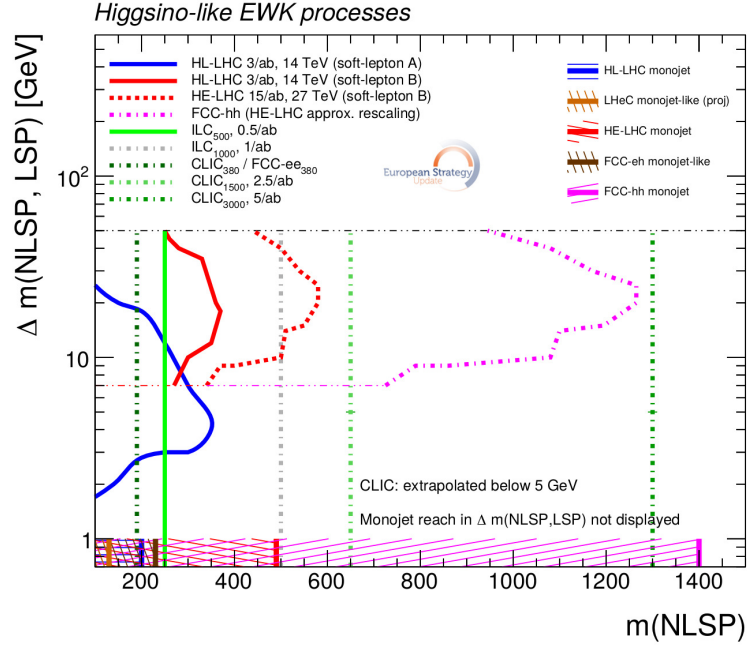


Figure 10: Properties of signal and background of  $\tilde{\chi}_1^\pm$  production. (a) Average  $m_{qq}$  in  $pp \rightarrow Zg \rightarrow \nu\bar{\nu}g$  versus  $M_{\tilde{\chi}_1^\pm}$  when the cut on the  $\nu\bar{\nu}$  transverse momentum is adjusted according to the expected missing transverse momentum of a  $\tilde{\chi}_1^\pm$ . It is set to  $0.85 M_{\tilde{\chi}_1^\pm}$ . (b) Cross-section of  $\tilde{\chi}_1^\pm$ -pair production (red-solid), together with that of  $pp \rightarrow Zg \rightarrow \nu\bar{\nu}g$  with cuts on the  $\nu\bar{\nu}$  increasing with  $M_{\tilde{\chi}_1^\pm}$  for three choices of  $\Delta(M)$ , keeping the cut at 75 % of the highest possible missing  $p_T$  for the signal: nominal (blue-solid, cut =  $0.85 M_{\tilde{\chi}_1^\pm}$ ),  $\frac{3}{4}\Delta(M)_{nom}$ . (blue-dotted, cut =  $0.7 M_{\tilde{\chi}_1^\pm}$ ), and  $\frac{1}{2}\Delta(M)_{nom}$ . (blue-dashed, cut =  $0.5 M_{\tilde{\chi}_1^\pm}$ ).

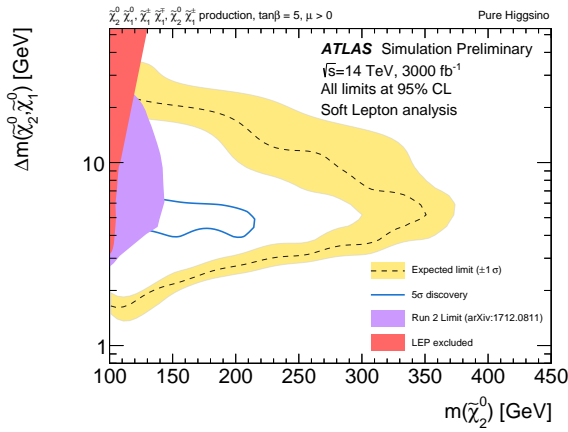
analysis must be done assuming the least favourable production-process and least favourable decay-mode. Finally, we pointed out that to extend the coverage to higher NLSP masses at constant LSP mass, while retaining the same signal efficiency can be done by making the cut on MET *stronger*, and that the signal-to-background ratio will remain constant when doing so. In contrast, to extend the coverage to higher LSP masses at constant NLSP mass (i.e. to lower  $\Delta(M)$ ) at constant signal efficiency, one must make the MET-cut *weaker*, and thus making the signal-to-background ratio lower. A lower MET-cut also implies that proportionally more background originates from fake MET due to detector effects, or from non-prompt neutrinos. The conclusion is that while progress with increased (parton) luminosity in the  $M_{NLSP}$  direction is substantial, the progress into the region of lower  $\Delta(M)$  will be much less pronounced.

## 4.2 Wino/Higgsino LSP

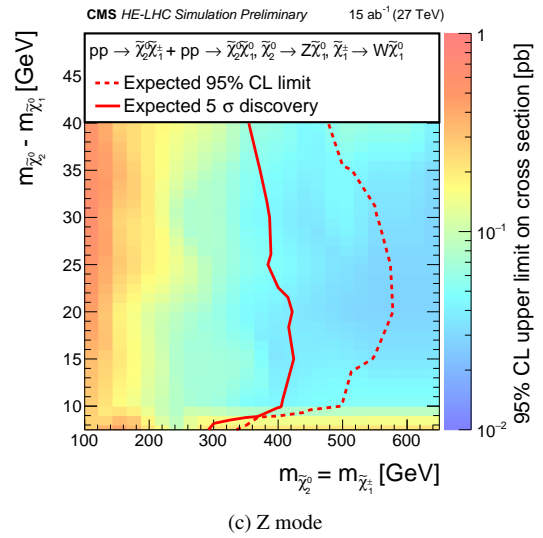
Figure 8.10 in [7] (reproduced here as Figure 11) shows the estimated reaches in the Wino or Higgsino LSP case, i.e. for the small  $\Delta(M)$  case. The two curves come from the HL-LHC projections from ATLAS [16] (solid blue) and CMS [17, 18] (solid red). In the CMS case, energy and luminosity scaling extrapolation to HE-LHC (dashed red) and FCChh (dashed magenta) are also done. Both collaborations make assumptions on the spectrum, however different ones: ATLAS assumes  $\Delta(M_{\tilde{\chi}_1^\pm}) = \Delta(M_{\tilde{\chi}_2^0})/2$ ,



(a) Z mode



(b) Z mode



(c) Z mode

Figure 11: The reaches in the low  $\Delta(M)$  (Higgsino- or Wino-LSP) region, as reported in [7] (top), and the two projections to HL-LHC from ATLAS [16] and CMS[17, 18] (bottom). (b) corresponds to the solid blue line in (a), (c) to the red line

while CMS assumes  $\Delta(M_{\tilde{\chi}_1^\pm}) = \Delta(M_{\tilde{\chi}_2^0})$ . In Figure 5a, the points in our scan that fulfil the ATLAS condition are marked with squares and those that fulfil CMS one are marked with triangles.

The reason for the sharp cut-off at low mass-differences, seen in 11a, is that these searches require leptonic decays of the NLSP to be possible to extract a signal from a huge, mainly hadronic, QCD background. Lepton identification is therefore essential, and this requires that the particle reaches the barrel calorimeters. The cut-off then appears because below this mass-difference, the decay products are so soft that they are bent back by the detector B-field inside the radius of the calorimeters. This cut-off would be at higher  $\Delta(M)$  at FCChh, since the reference detector design [20] foresees a considerably larger inner radius of the barrel calorimeter system ( $\sim 2$  m, while ATLAS and CMS have an inner radius of 1.5 m and 1.3 m, respectively), and a stronger B-field (4 T vs. 2(3.8) T for ATLAS(CMS)). From this, one also sees that the CMS properties are closer to the FCChh detector in this respect: cut-off

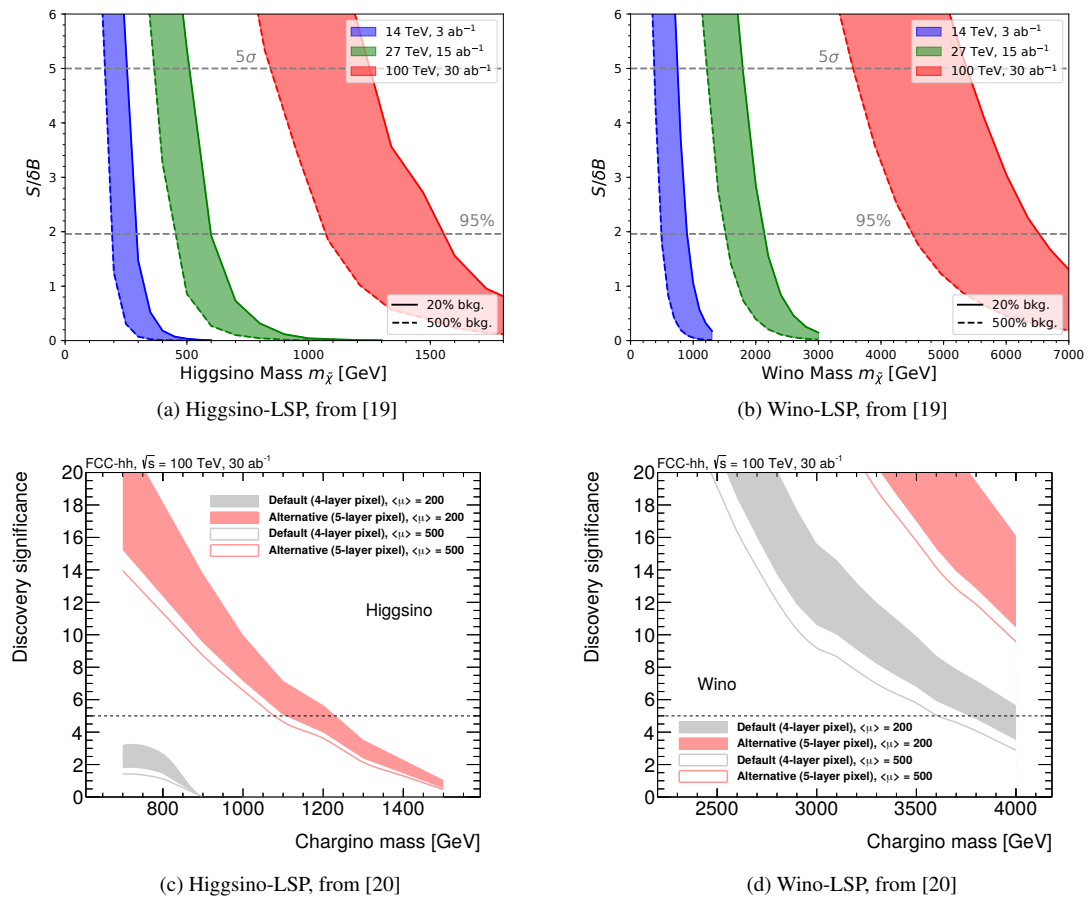


Figure 12: The sensitivities for the “Disappearing tracks” at future pp-colliders. In (c) and (d), the grey bands corresponds to the actual FCChh conceptual detector.

transverse momenta are 1.2, 0.7 and 0.4 GeV for FCChh, CMS and ATLAS, respectively. In addition, the analyses use the combination of NLSP-NLSP, NLSP-NNLSP and NNLSP-NNLSP production, and assume certain relations between the mass difference to the LSP of the NLSP or NNLSP, different for ATLAS and CMS, as mentioned above. Our scan shows that these relations are quite particular cases. Whether these assumptions are essential or not is an open question, but we do conclude that the soft-lepton analysis will progress to higher NLSP masses, but not to lower  $\Delta(M)$ , and remains model-dependent.

The hatched band at the bottom of Figure 11a shows the reach at very low  $\Delta(M)$ . The upper edge of the band at  $\Delta(M)=1$  GeV should not be taken literally; only the reach in  $M_{LSP}$  is relevant. Two methods are used to estimate the reach at very low  $\Delta(M)$ : “Disappearing tracks” and “Mono-

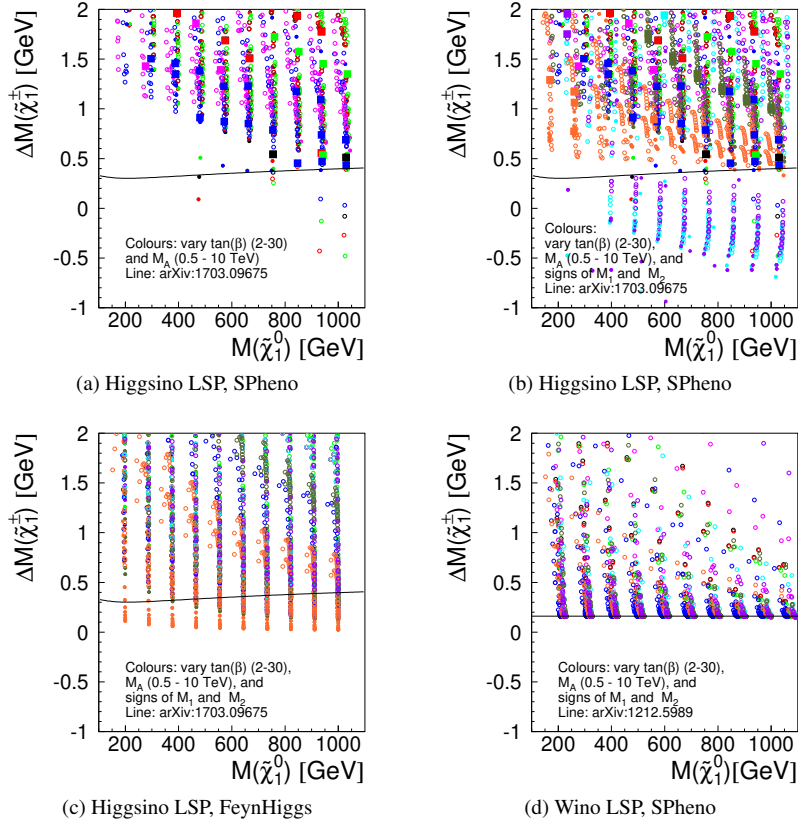


Figure 13: Zoom-in of Figure 5, showing  $\Delta(M_{\tilde{\chi}_1^\pm})$  vs.  $M_{LSP}$  in the small  $\Delta(M)$  region. In (a) only models with  $\mu$ ,  $M_1$ , and  $M_2$  all positive are shown. In (b) and (c) all models are shown, for both spectrum calculation codes we used. The lines are from [21] (a,b,c) and [22](d), and are the mass-differences used in the calculation of the reaches shown in Figures 12 and 15. In (a) and (b), the squares are points where  $\Delta(M_{\tilde{\chi}_1^\pm}) = \Delta(M_{\tilde{\chi}_2^0})/2$ , i.e. the “deep Higgsino” region; the colours are explained in Figure 3.

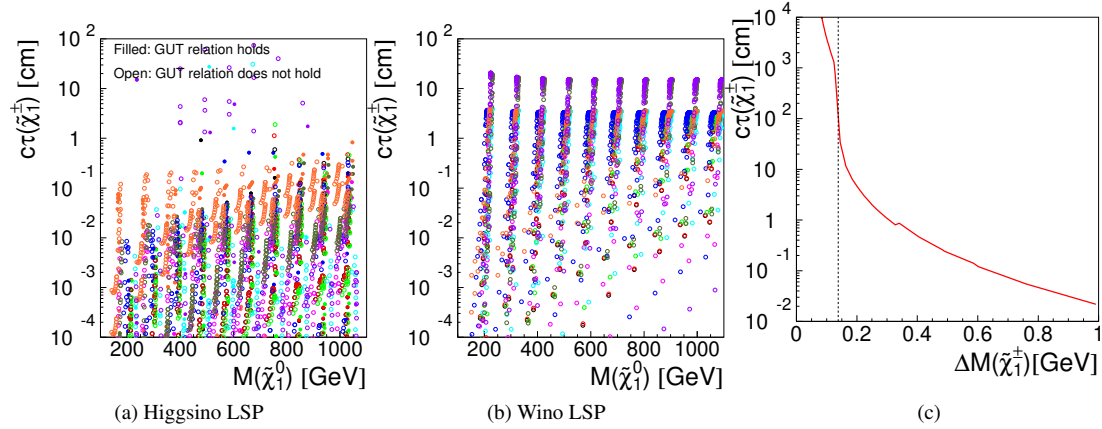


Figure 14:  $c\tau(\tilde{\chi}_1^\pm)$  vs.  $M_{LSP}$  for Higgsino (a) and Wino (b) LSP, and  $c\tau(\tilde{\chi}_1^\pm)$  vs.  $M_{\tilde{\chi}_1^\pm}$  for Higgsino LSP (c). Colours as explained in Figure 3.

X”. The “Disappearing tracks” signature, which consists of a topology where a reconstructed trajectory terminates inside the tracking volume, indicating that a decay took place where the decay product had a momentum below the threshold of detectability. This signature is effective for cases with low mass-differences, since this potentially implies both a long lifetime of the primary NLSP, and little energy release in it’s decay. The “Mono-X” technique is effective if the decay products of the produced bosinos are so soft that they are invisible, or if only LSP-pairs are produced. One then searches for the a large unbalanced  $p_T$  from an initial state radiation, which could be a gluon, photon,  $Z$ ,  $W$  or  $h$ . In pp-collisions, the gluon would be the prime candidate.

The “Disappearing tracks” method was used by FCChh (in the CDR[20]), as well as in [19]. The two results are shown in Figure 12. The upper row is from [19], while the lower row is from [20]. In the latter, the grey curves should be considered: the pink ones shows what could be obtained if the innermost layer of the vertex detector would be placed much closer to the beam than what is assumed to be the closest conceivable radius, given the radiation levels expected [20]. One can observe a large discrepancy between the results in the upper and lower row in the figure. Both are based on Delphes parameterised fast simulation [23], but the FCChh analysis is more realistic, in that it assumes a detector as assumed in the CDR, and with a more FCChh-like number of pile-up events (even though it only assumes a pile-up of 500, rather than the number 955 that is stated elsewhere in the CDR). The analysis of [19] simply uses the current ATLAS setup of Delphes, presumably meaning a pile-up level of LHC, which is some 20 times lower than that foreseen at FCChh. It should be noted that the CDR detector (the grey bands) has its closest layer closer than that of the current ATLAS, and should actually be more powerful than ATLAS, in stark contrast with what is seen. One observes that for Higgsinos, the significance of a signal only barely reaches two sigma. This is quite different from what is found in [19], and reflects more realistic simulation would yield.

The key element for the “Disappearing tracks” analysis is the magnitude of  $\Delta(M)$ . Figure 13a,b is a zoom in of Figure 5a, showing the Higgsino LSP case. In the figure the absolute lower limit of  $\Delta(M)$  mentioned in the Briefing-book, which was given in [21], is also shown. Figure 13a shows



models where  $\mu$ ,  $M_1$  and  $M_2$  are all positive. In this case, the lower limit is respected, but reached only for few models. Figure 13b shows the situation after the full scan where any combinations of signs of  $\mu$ ,  $M_1$  and  $M_2$  is allowed. Clearly the limit is violated, and this is because the calculation in [21] only refers to  $SM$  effects on the mass-splitting, assuming that mixing effects between the SUSY fields are negligible. This situation occurs in the “deep Higgsino” region where  $M_1$  and  $M_2 \gg \mu$ . In Figure 4b, the models that are in this region are those that lies on the line labelled “Pure Higgsino line”. One also notes that many models, in particular those where  $\mu$  is negative, features a chargino LSP. As already mentioned, `SPheno` and `FeynHiggs` give different results in this case, and Figure 13c shows the spectrum under the same conditions as in Figure 13b, but calculated with `FeynHiggs` rather than `SPheno`. One sees that `FeynHiggs` does not yield chargino LSPs, but does not seem to respect the limiting mass-difference. This observation is interesting, but not essential for the question of guaranteed exclusion: The important feature in this respect is that there *are* models with  $\Delta(M) = 1$  GeV and above at all  $M_{LSP}$ , i.e. far above what is reachable with the “Disappearing tracks” method, and that the two codes agree on this. In Figure 13d, the corresponding zoom of Figure 5b is shown, and illustrates the Wino LSP case. The line in 13d is the lower limit given in [22], which as can be seen is respected, but is by no means attained by all models. It is also worth mentioning that the Wino LSP scenario, by it’s very construction, does not allow for GUT-scale  $M_1$ - $M_2$  unification.

For the “Disappearing track” analysis, the decay-length needs to be macroscopic. In [24], the ATLAS collaboration reported their results on this type of search at 13 TeV. They found that the search is effective for lifetimes of about 200 ps, corresponding to a  $c\tau$  of about 6 cm. Figure 14 shows  $c\tau$  for the different considered models. One can see that in the Higgsino case, hardly any points in our scan would yield a decay-length long enough - in fact most of the models have a  $c\tau$  below 1 mm. In the Wino LSP case, on the other hand, there are good chances that  $c\tau$  would be 1 cm or more. There are, however, even in this case models where  $c\tau$  is below 1 mm, so a non-observation of a signal cannot be used to infer that the Wino LSP hypothesis is excluded. In Figure 14c, the dependence of  $c\tau$  on  $\Delta(M)$  for a Higgsino LSP is shown. One can note that  $c\tau$  becomes above 1 mm only for  $\Delta(M)$  less than 600 MeV, so in fact the excluded region from disappearing tracks is off the vertical scale in Briefing-book Figure

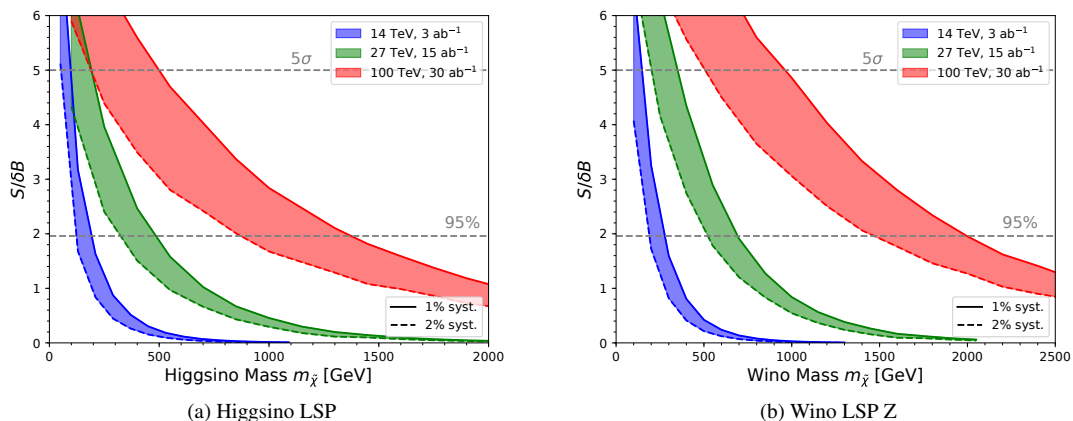


Figure 15: The sensitivities for the “Mono-X” technique at future pp-colliders. From [19].



11.

For the “Mono-X” signature, the source of the limits is [19], and the key figures from that publication are shown in Figure 15. It should be noted that these figures were included in the HE/HL-LHC input to ESU [25], not the FCChh one [26], nor in the FCChh CDR [20]. As mentioned above, the analysis is based on Delphes fast simulation using the ATLAS-card, and we saw that when applied to the “Disappearing tracks” it gave results far better than those of the more realistic analysis in the FCChh CDR. Furthermore, by scrutinising the dependence of the significance of a signal versus the mass and assumed systematic errors, one can conclude that the results are systematics limited, with systematics assumed to be between 1 and 2 %. This can be contrasted to existing “Mono-X” analyses from both ATLAS [27] and CMS [28], which both estimate systematic errors at the level of 10 %, with a pile-up 20 times lower than that expected at FCChh. It is also noteworthy that there to date are no results from ATLAS nor CMS where their “Mono-X” searches have been used to infer any conclusions about SUSY.

## 5 Summary of the ILC projections

In this section, we make a brief summary of the expected performance of the SUSY searches at the ILC. A more comprehensive account can be found in [33–35]. Figure 16, from [29], shows the reach of an 500 GeV ILC in the search for  $\tilde{\chi}_1^\pm$  in the Higgsino- and Wino-LSP cases. These projections were obtained by extrapolation of the LEP II results [2], using background-levels and signal-efficiencies as reported in [2], assuming no other ameliorations over LEP II than increased beam energy, beam-polarisation, and data set size. This is clearly a very conservative assumption as it neglects the progress

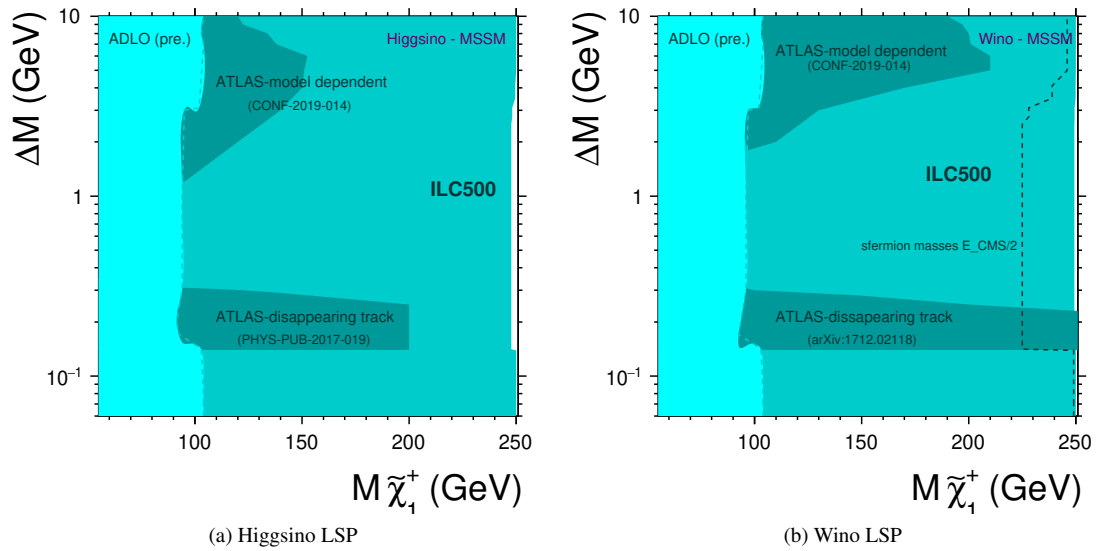


Figure 16: Exclusion reaches for  $\tilde{\chi}_1^\pm$  at LEP II [2], ILC-500 [29], and LHC [24, 30, 31]. The LEP II, ILC, and ATLAS “disappearing tracks” analyses are valid without any assumption, while the ATLAS “soft leptons” assumes  $M_1$  and  $M_2 \gg \mu$

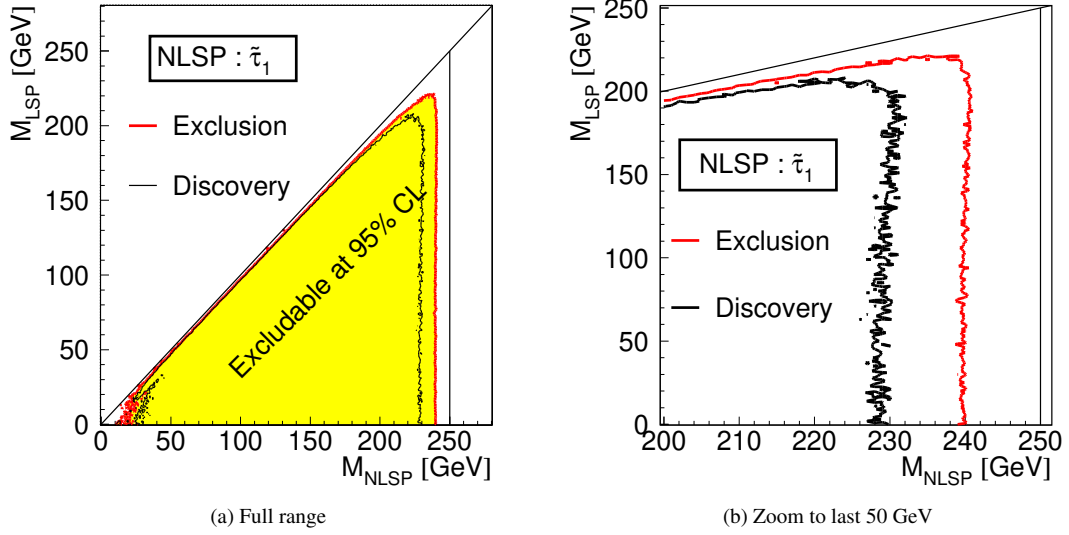


Figure 17: Reach at ILC-500 for the  $\tilde{\tau}$  NLSP case. From [32]

in detector technology, reported in volume 4 of the ILC TDR [36]. In [29], it is shown that if  $\Delta(M) > 3$  GeV, exclusion and discovery-reach are only a few 100 MeV apart, and if  $\Delta(M)$  is between 3 GeV and  $m_\pi$ , they are at most 5 GeV from each other. The only caveat is in a very particular situation where

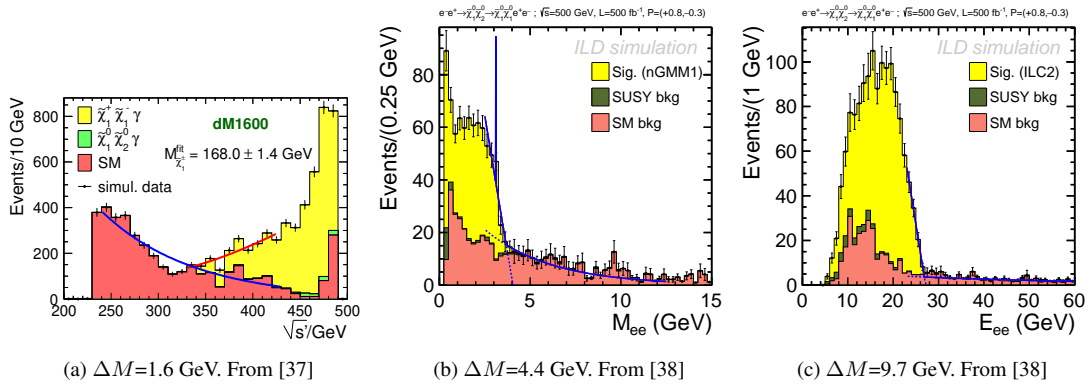


Figure 18: Examples of Higgsino signals at ILC-500, and various models and mass-differences. The assumed integrated luminosity is  $500 \text{ fb}^{-1}$  in all cases. In (a)  $\tilde{\chi}_1^\pm$  is the NLSP, in (b) and (c) it is the  $\tilde{\chi}_1^0$ . The spike in (b) is the  $J/\Psi$ .

destructive interference between the s-channel and the sneutrino-induced t-channel could reduce the production cross-section drastically for the Wino-LSP case [39]. This only happens when the sneutrino mass is close to the beam-energy, and in most of that parameter-space, the sneutrino, not the  $\tilde{\chi}_1^\pm$ , is the NLSP. The experimental implications of such a low mass sneutrino were not studied<sup>4</sup>.

Even in this case, exclusion is guaranteed up to  $M_{\tilde{\chi}_1^\pm}=246$  GeV, discovery to 243 GeV, if  $\Delta(M) > 3$  GeV. There is a substantial loss of reach only in the region where  $\Delta(M)$  is between 3 GeV and  $m_\pi$ , where exclusion is guaranteed up to  $M_{\tilde{\chi}_1^\pm}=225$  GeV, discovery to 205 GeV. However, one should keep in mind that the main reason for the drop in efficiency at LEP II in this  $\Delta(M)$  region was trigger-efficiency, and the ILC detectors are to be run trigger-less. In [32], a SUSY parameter scan using detailed fast simulation of the ILD at ILC was done, to establish the reach in the experimentally worst case NLSP, namely the  $\tilde{\tau}_1$  with the mixing angle in the  $\tilde{\tau}$  sector that minimises the production cross-section. The results are shown in Figure 17, showing that also in this case, exclusion (discovery) is possible to 10 (20) GeV below the kinematic limit, already a modest integrated luminosity of  $500 \text{ fb}^{-1}$ , less than a third of what is expected at the favourable beam-polarisation settings (*viz.* right-handed electron, left-handed positron). One can note that the limits are valid only if  $\Delta(M) > 3\text{-}4$  GeV, however no dedicated low  $\Delta(M)$  analysis was done in [32] - it is the subject of an ongoing study. The same publication also studied the arguably most favourable NLSP candidate, the smuon, and found that exclusion (discovery) would be assured at 2(4) GeV below the kinematic limit. Several full simulation studies have been done at particular Higgsino-LSP model-points, typically with modest to very low  $\Delta(M)$  [37, 38]. A few examples are shown in Figure 18, and illustrate how clean the signal is expected to be.

## 6 Summary and Conclusions

We have discussed the landscape of possible MSSM models that could have a next-to-lightest SUSY particle (an NLSP) in reach of future HEP facilities. We have concentrated on the case of an electroweak bosino NLSP, as this in almost all cases is the most challenging one, in addition to being quite likely. In doing so, we scanned over a grid of values of  $\mu$ ,  $M_1$ , and  $M_2$ , with the only constraint that the NLSP should not be heavier than a few TeV. We did *not* require that the models contained a viable dark matter candidate, solved the naturalness problem, gave an explanation to the g-2 anomaly, etc, nor that there were any particular relations between the parameters. In this way, the study carries no prejudice on any SUSY breaking scheme, nor the possible existence of other beyond the standard model phenomena. We confronted our findings on possible spectra, cross-sections and decay branching-ratios to projections done for the various options for future facilities, taking into consideration the detail and maturity of both the projects and the individual analyses. We concentrated on future pp-colliders, in particular FCChh, only briefly touching upon the  $e^+e^-$ -colliders (mainly because the conclusion about the latter are very simple: either discovery or exclusion is guaranteed up a few GeV below the kinematic limit, under all circumstances).

For the high  $\Delta(M)$  *Bino-region*, the signal at pp-colliders is unambiguous, in the sense that it consists of missing transverse momentum (MET), originating from the invisible SUSY particles themselves, without need for a system recoiling against the SUSY particles. We note, however, that the relative contributions from different possible processes can vary over a large range, as can the decay branching ratios. Since the sensitivity of the analyses depends on this, to claim exclusion one must establish which of these yields the lowest sensitivity. This is usually not done, but rather a single representative model is assumed. A further observation is that there is a simple scaling of the reach to be expected (Sect. 4.1),

<sup>4</sup>In [40], a theoretical study of this situation was undertaken. The experimental issues will be a topic for future studies.

which is corroborated by the data at LHC at 7 and 13 TeV respectively, and the thorough HL-LHC projections. This leads to the expectation that the reach will be extended far at the highest mass-differences, while only modest progress can be hoped for to lower mass-differences. Models currently excluded are only such where unification of  $M_1$  and  $M_2$  at the GUT-scale does not occur - only little progress can be expected into the region where GUT-scale unification is possible.

For the low  $\Delta(M)$  region, the *Wino*- and *Higgsino*- regions, the MET from SUSY itself is too small to consist a signal-signature, and more channel-specific searches are needed, in conjunction with the presence of a sizeable system recoiling against the SUSY particles. At mass-differences down to a few GeV, leptonic decays can be searched for. Due to the need for lepton-identification, this method will not be able to reach as low mass differences at FCChh as what is attained at LHC. At mass differences an order of magnitude lower, the lifetime of the NLSP might become big enough that its decay in the detector would be observable (the “Disappearing track” technique). FCChh prospects for Higgsinos with this technique are not promising, while they are for Winos. This is due to the expected lower mass-differences in the latter case. In existing analyses from ATLAS and CMS of both these techniques, as well as in the projections, very specific model-points have been assumed, usually corresponding to situations where the mass-splitting is only due to SM loop-effects, ignoring the effects of mixing in the SUSY sector. Our parameter-scan shows that these assumptions are quite aggressive, and completely different mass-spectra are common-place. In fact, with one of the spectrum calculators we used, some models actually acquire a  $\tilde{\chi}_1^\pm$  LSP.

A second technique to probe  $\Delta(M)$  below the cut-off of the soft-lepton technique is the “Mono-X” one, where the decay of the NLSP is assumed to be undetectable, and the signal would be the presence of a high  $P_T$  mono-jet (or photon, Z, W or higgs), recoiling against an invisible system. The power of this technique has not been evaluated to a level that allows for any conclusions, nor has it been used by ATLAS or CMS in a SUSY context.

In conclusion, future pp-colliders do have a large *discovery reach*, where it is permissible to assume that the model realised in nature is *favourable*. However, the *exclusion reach*, where one must assume that the model realised is the *least favourable*, is quite modest, and has not been evaluated in large detail. Notwithstanding the gaps in finding the least favourable model, one can already note that the regions where the mass-differences are considerable, but still small enough to allow models with GUT-scale  $M_1$ - $M_2$  unification will to a large extent remain uncovered. Furthermore, the low mass-difference regions leaves gaps both above and below the region that the soft-lepton method can cover, regions where both Higgsino- and Wino-LSP models thrive. A window of opportunity exists at very small differences, but only for very specific models.

None of these shortcomings are present for future TeV-scale  $e^+e^-$  colliders. At these facilities, SUSY will be excluded or discovered up to the kinematic limit, under all circumstances, and remain *the* option to exhaustively test the hypothesis of weak-scale SUSY.

## References

- [1] (a) J. Wess, B. Zumino, Nucl. Phys. **B70** (1974), [24(1974)] 39; (b) H. P. Nilles, Phys. Rept. **110** (1984) 1; (c) H. E. Haber, G. L. Kane, Phys. Rept. **117** (1985) 75; (d) R. Barbieri, S. Ferrara, C. A. Savoy, Phys. Lett. **119B** (1982) 343.
- [2] ALEPH, DELPHI, L3 and OPAL experiments, *LEPSUSYWG, Reports 04-01.1, 04-02.1, 01-03.1, and 02.-04.1*, 2004, URL: <http://lepsusy.web.cern.ch/lepsusy/Welcome.html>.

- [3] (a) A. Heister et al., Phys. Lett. **B526** (2002) 206, arXiv: hep-ex/0112011 [hep-ex]; (b) A. Heister et al., Phys. Lett. **B583** (2004) 247; (c) A. Heister et al., Phys. Lett. **B533** (2002) 223, arXiv: hep-ex/0203020 [hep-ex].
- [4] J. Abdallah et al., Eur. Phys. J. **C31** (2003) 421, arXiv: hep-ex/0311019 [hep-ex].
- [5] P. Achard et al., Phys. Lett. **B580** (2004) 37, arXiv: hep-ex/0310007 [hep-ex].
- [6] G. Abbiendi et al., Eur. Phys. J. **C32** (2004) 453, arXiv: hep-ex/0309014 [hep-ex].
- [7] R. K. Ellis et al., (2019), arXiv: 1910.11775 [hep-ex].
- [8] (a) E. Bagnaschi et al., Eur. Phys. J. **C78** 3 (2018) 256, arXiv: 1710.11091 [hep-ph]; (b) E. Bagnaschi et al., *Global SM and BSM Fits using Results from LHC and other Experiments*, Particles, Strings and the Early Universe: The Structure of Matter and Space-Time, ed. by J. Haller, M. Grefe, 2018, p. 203; (c) S. Caron et al., Eur. Phys. J. **C77** 4 (2017) 257, arXiv: 1605.02797 [hep-ph]; (d) G. Aad et al., JHEP **10** (2015) 134, arXiv: 1508.06608 [hep-ex].
- [9] D. J. E. Marsh, Phys. Rept. **643** (2016) 1, arXiv: 1510.07633 [astro-ph.CO].
- [10] M. Abdughani, L. Wu, Eur. Phys. J. **C80** 3 (2020) 233, arXiv: 1908.11350 [hep-ph].
- [11] (a) W. Porod, Comput. Phys. Commun. **153** (2003) 275, arXiv: hep-ph/0301101 [hep-ph]; (b) W. Porod, F. Staub, Comput. Phys. Commun. **183** (2012) 2458, arXiv: 1104.1573 [hep-ph].
- [12] (a) W. Kilian, T. Ohl, J. Reuter, Eur. Phys. J. **C71** (2011) 1742, arXiv: 0708.4233 [hep-ph]; (b) M. Moretti, T. Ohl, J. Reuter, (2001) 1981, arXiv: hep-ph/0102195 [hep-ph].
- [13] (a) H. Bahl et al., Comput. Phys. Commun. **249** (2020) 107099, arXiv: 1811.09073 [hep-ph]; (b) H. Bahl et al., Eur. Phys. J. **C78** 1 (2018) 57, arXiv: 1706.00346 [hep-ph]; (c) H. Bahl, W. Hollik, Eur. Phys. J. **C76** 9 (2016) 499, arXiv: 1608.01880 [hep-ph]; (d) T. Hahn et al., Phys. Rev. Lett. **112** 14 (2014) 141801, arXiv: 1312.4937 [hep-ph]; (e) M. Frank et al., JHEP **02** (2007) 047, arXiv: hep-ph/0611326 [hep-ph]; (f) G. Degrossi et al., Eur. Phys. J. **C28** (2003) 133, arXiv: hep-ph/0212020 [hep-ph]; (g) S. Heinemeyer, W. Hollik, G. Weiglein, Eur. Phys. J. **C9** (1999) 343, arXiv: hep-ph/9812472 [hep-ph]; (h) S. Heinemeyer, W. Hollik, G. Weiglein, Comput. Phys. Commun. **124** (2000) 76, arXiv: hep-ph/9812320 [hep-ph].
- [14] *Prospects for searches for staus, charginos and neutralinos at the high luminosity LHC with the ATLAS Detector*, tech. rep. ATL-PHYS-PUB-2018-048, Geneva: CERN, 2018, URL: <https://cds.cern.ch/record/2651927>.
- [15] J. Pumplin et al., JHEP **07** (2002) 012, arXiv: hep-ph/0201195 [hep-ph].
- [16] *ATLAS sensitivity to winos and higgsinos with a highly compressed mass spectrum at the HL-LHC*, tech. rep. ATL-PHYS-PUB-2018-031, Geneva: CERN, 2018, URL: <https://cds.cern.ch/record/2647294>.
- [17] A. M. Sirunyan et al., Phys. Lett. **B782** (2018) 440, arXiv: 1801.01846 [hep-ex].
- [18] *Searches for light higgsino-like charginos and neutralinos at the HL-LHC with the Phase-2 CMS detector*, tech. rep. CMS-PAS-FTR-18-001, 2018.
- [19] T. Han, S. Mukhopadhyay, X. Wang, Phys. Rev. **D98** 3 (2018) 035026, arXiv: 1805.00015 [hep-ph].
- [20] A. Abada et al., Eur. Phys. J. ST **228** 4 (2019) 755.
- [21] H. Fukuda et al., Phys. Lett. **B781** (2018) 306, arXiv: 1703.09675 [hep-ph].

- [22] M. Ibe, S. Matsumoto, R. Sato, Phys. Lett. **B721** (2013) 252, arXiv: 1212.5989 [hep-ph].
- [23] J. de Favereau et al., JHEP **02** (2014) 057, arXiv: 1307.6346 [hep-ex].
- [24] M. Aaboud et al., JHEP **06** (2018) 022, arXiv: 1712.02118 [hep-ex].
- [25] A. Dainese et al., *The physics potential of HE-LHC*, 2019, URL: <https://indico.cern.ch/event/765096/contributions/3296016/attachments/1785350/2906423/HELHC.pdf>.
- [26] M. Benedikt et al., *Future Circular Collider The Hadron Collider (FCC-hh)*, 2019, URL: [https://indico.cern.ch/event/765096/contributions/3298184/attachments/1786069/2907901/133\\_ESPP18\\_FCChh\\_181115-FCC\\_V0600\\_MainText.pdf](https://indico.cern.ch/event/765096/contributions/3298184/attachments/1786069/2907901/133_ESPP18_FCChh_181115-FCC_V0600_MainText.pdf).
- [27] M. Aaboud et al., JHEP **01** (2018) 126, arXiv: 1711.03301 [hep-ex].
- [28] (a) S. Chatrchyan et al., JHEP **09** (2012) 094, arXiv: 1206.5663 [hep-ex]; (b) A. M. Sirunyan et al., Phys. Rev. **D97** 9 (2018) 092005, arXiv: 1712.02345 [hep-ex].
- [29] M. T. Núñez Pardo de Vera, M. Berggren, J. List, *Chargino production at the ILC*, International Workshop on Future Linear Colliders (LCWS 2019) Sendai, Miyagi, Japan, October 28-November 1, 2019, 2020, arXiv: 2002.01239 [hep-ph].
- [30] G. Aad et al., (2019), arXiv: 1911.12606 [hep-ex].
- [31] *Search for direct pair production of higgsinos by the reinterpretation of the disappearing track analysis with  $36.1 \text{ fb}^{-1}$  of  $\sqrt{s} = 13 \text{ TeV}$  data collected with the ATLAS experiment*, tech. rep. ATL-PHYS-PUB-2017-019, Geneva: CERN, 2017, URL: <https://cds.cern.ch/record/2297480>.
- [32] M. Berggren, *Simplified SUSY at the ILC*, Proceedings, 2013 Community Summer Study on the Future of U.S. Particle Physics: Snowmass on the Mississippi (CSS2013): Minneapolis, MN, USA, July 29-August 6, 2013, 2013, arXiv: 1308.1461 [hep-ph].
- [33] P. Bambade et al., (2019), arXiv: 1903.01629 [hep-ex].
- [34] K. Fujii et al., (2017), arXiv: 1702.05333 [hep-ph].
- [35] M. Berggren et al., *Electroweakino Searches: A Comparative Study for LHC and ILC (A Snowmass White Paper)*, Proceedings, 2013 Community Summer Study on the Future of U.S. Particle Physics: Snowmass on the Mississippi (CSS2013): Minneapolis, MN, USA, July 29-August 6, 2013, 2013, arXiv: 1309.7342 [hep-ph].
- [36] H. Abramowicz et al., (2013), ed. by T. Behnke et al., arXiv: 1306.6329 [physics.ins-det].
- [37] M. Berggren et al., Eur. Phys. J. **C73** 12 (2013) 2660, arXiv: 1307.3566 [hep-ph].
- [38] H. Baer et al., (2019), arXiv: 1912.06643 [hep-ex].
- [39] S. Y. Choi et al., Eur. Phys. J. **C7** (1999) 123, arXiv: hep-ph/9806279 [hep-ph].
- [40] G. A. Moortgat-Pick, H. Fraas, Acta Phys. Polon. **B30** (1999) 1999, arXiv: hep-ph/9904209 [hep-ph].